

## Article

# Flame Retardancy Performance of Continuous Glass-Fiber-Reinforced Polypropylene Halogen-Free Flame-Retardant Prepreg

Yiliang Sun <sup>1</sup>, Jingwen Li <sup>1,\*</sup> and Hongfu Li <sup>2</sup>

<sup>1</sup> School of Materials Science and Engineering, Beihang University, Beijing 100191, China; ylsun@buaa.edu.cn

<sup>2</sup> School of Materials Science and Engineering, University of Science and Technology Beijing, Beijing 100083, China; lihongfu@ustb.edu.cn

\* Correspondence: ljh666@buaa.edu.cn

**Abstract:** Thermoplastic resin matrix has a high melt viscosity, which is difficult to impregnate with fibers. The addition of flame retardant will further increase the viscosity of the melt and increase the difficulty of impregnation. It is possible to reduce the effect of flame retardant on melt viscosity by adding high-flow polypropylene. In this study, the effect of adding flame retardant on the impregnation quality of prepreg tape was investigated. By adding high-flow polypropylene to improve the melt viscosity of flame-retardant-modified polypropylene, continuous glass-fiber-reinforced polypropylene flame-retardant prepreg tape was successfully prepared. Intumescence flame retardant (IFR) was added at 20 wt%, 25 wt%, 30 wt% of the polypropylene matrixes, which were prepared by melt impregnation. The composites were analyzed with thermogravimetric analysis, limiting oxygen index testing, UL-94 flame retardancy testing, cone calorimeter testing (CCT) and scanning electron microscopy. Tests involving the flame retardant showed that when the added amount of flame retardant reached 25%, the UL-94 flame retardancy grade reached V0. Compared with the CCT sample heating data, taking economic considerations into account, 25 wt% IFR addition was the most suitable.

**Keywords:** polypropylene; continuous glass fiber; intumescence flame retardant; unidirectional prepreg; thermoplastic composites



**Citation:** Sun, Y.; Li, J.; Li, H. Flame Retardancy Performance of Continuous Glass-Fiber-Reinforced Polypropylene Halogen-Free Flame-Retardant Prepreg. *Coatings* **2022**, *12*, 976. <https://doi.org/10.3390/coatings12070976>

Academic Editors: Giulio Malucelli and Pavel Košťál

Received: 30 April 2022

Accepted: 6 July 2022

Published: 9 July 2022

**Publisher's Note:** MDPI stays neutral with regard to jurisdictional claims in published maps and institutional affiliations.



**Copyright:** © 2022 by the authors. Licensee MDPI, Basel, Switzerland. This article is an open access article distributed under the terms and conditions of the Creative Commons Attribution (CC BY) license (<https://creativecommons.org/licenses/by/4.0/>).

## 1. Introduction

Continuous fiber-reinforced thermoplastic composites (CFRTPs) exhibit greatly improved mechanical properties and have a wide range of applications. CFRTPs are very promising materials for use in the automotive industry, rail transport, the aviation industry, and other fields, because they have no storage-cycle limitations, short molding cycles, and are recyclable. [1] Polypropylene (PP) has been widely used in thermoplastic matrices because of its low molding temperature, good chemical stability, excellent comprehensive performance, and low price. Continuous fiber-reinforced PP composite materials account for a large proportion of continuous fiber-reinforced thermoplastic composite materials; however, the flammability of PP is a problem that extends to continuous fiber-reinforced PP composite materials, and needs to be resolved in order to expand their field of application [2,3].

Many studies have been conducted on the addition of flame retardants to PP to restrict its flammability [4–10]. Among the commonly used flame retardants for PP, intumescence flame retardants (IFRs) have a high flame-retardant efficiency for relatively low loadings [9,11–16]. Moreover, as they have little impact on the mechanical properties of the PP matrix, and satisfy the halogen-free environmental protection requirements, IFRs have been subject to considerable research and use in many applications. Research about the addition of IFRs into discontinuous glass-fiber-reinforced PP composites is increasing,

while research around IFR addition into continuous fiber-reinforced PP composites remains relatively limited [17–20]. With respect to the study of glass-fiber-reinforced polypropylene flame-retardant materials, the impact of the glass fibers can be considered from two perspectives. On one hand, during the combustion progress of the PP matrix, the PP melt accelerates along the fiber direction with the flame. Because the glass fiber plays a role similar to a candle wick, this phenomenon is called the candlewick effect [21–23]. On the other hand, glass fibers are noncombustible. As a reinforcing material, glass fibers can be used in combination with flame retardants to increase the flame retardant and mechanical properties of PP [23–25]. The addition of IFR can effectively weaken the wick effect. This can ensure not only the flame retardant effect, but also the mechanical properties.

From the perspective of composites material preparation [26–28], there are two processes for the preparation of continuous glass-fiber-reinforced flame-retardant composite materials. One is the flame-retardant modification of the PP matrix, which forms the basis of the glass-fiber-reinforced PP flame-retardant composite material. The other is the subsequent impregnation of continuous glass fibers into the flame-retardant PP matrix. According to the different impregnation processes, the preparation of continuous fiber-reinforced PP prepreg tapes can be divided into various methods: melting, solution, in situ, powder, commingled fibers, and film stack [29–34]. Among these, melt impregnation is the most widely used process due to its advantages of simple operation, facilitation of continuous production, a non-polluting production process, and reduced impact on the operator. The current theory governing resin-impregnated fibers is based on Darcy's law, from which a simplified impregnation model can be obtained:

$$s = \sqrt{\frac{2K\Delta p t}{\eta}},$$

where  $s$  represents the penetration depth,  $K$  is the permeability coefficient,  $\Delta p$  is the pressure drop in the melt flow direction,  $t$  is the impregnation time, and  $\eta$  is the viscosity of the fluid. From this equation several important parameters that affect the impregnation quality can be identified. The viscosity is an important characteristic of the thermoplastic melt, which is affected by the temperature and the amount of flame retardant added. In particular, the addition of a flame retardant increases the melt viscosity, which affects the quality of impregnation. During the resin impregnation of fiber bundles, the viscosity characteristics of the resin and the dense packing characteristics of the fiber bundles result in the formation of tiny voids in the molded prepreg tape. The volume percentage of voids is called the porosity, and characterizes the impregnation quality of the prepreg. The melt flow index (MFI) can characterize the effect of the added flame retardant and temperature on the viscosity and fluidity of the resin melt. The MFI represents the quality of the resin flowing through small holes under a certain pressure within a certain time period in the melt state, and its magnitude can be used to compare intuitively the difference in the resin melt's fluidity under different temperatures and with different flame retardant loadings. The preparation of continuous glass-fiber-reinforced PP flame-retardant prepreg tape requires balancing the amount of PP matrix, flame retardant, and impregnation quality. For example, a low amount of added IFR may not meet the flame-retardancy requirements, while a larger amount may significantly increase the melt viscosity, thus reducing fluidity and preventing good impregnation. In the existing literature, there is no research on the influence of IFR addition on the molding quality of continuous fiber-reinforced PP prepreg tapes.

In this study, the flame-retardant-modified polypropylene matrix was adjusted via the addition of high-fluidity polypropylene and temperature control. The impregnation of continuous glass fibers with the flame-retardant-modified polypropylene matrix containing different IFR additions was observed at different temperatures by measuring the porosity of flame-retardant unidirectional prepreg tape. The effects of different IFR loadings on flame retardancy were compared using the flame retardant performance test, and the IFR loading

and related prepreg tape preparation condition parameters were determined according to the prepreg preparation process.

## 2. Materials and Methods

### 2.1. Raw Materials

PP (bx3900) with a melt flow index of 60 g/10 min (2.16 kg at 230 °C) was provided by the SK Group, Seoul, South Korea; PP (MF650X) with a melt flow index of 1200 g/min (2.16 kg at 230 °C) was provided by the LyondellBasell corporation, Dalian, China; maleic anhydride grafted polypropylene (MAPP; Exxelor PO 1020) was obtained from the Exxon Mobil corporation, Shanghai, China; and glass fiber direct rovings (4305S) were supplied by the Chongqing Polycomp International corporation, Chongqing, China; the intumescence flame retardant (IFR) was obtained from the XinXiu corporation, Yantai, China, composed of ammonium polyphosphate, pentaerythritol, and melamine. The N content of the IFR was (21 ± 1)%), and its P content was (23 ± 1)%.

### 2.2. Preparation of Flame Retardant Modified Polypropylene

According to previous research on IFR-based flame-retardant PP, the flame-retardant mechanism of IFR arises from the formation of an expanded carbon layer during the combustion of PP, isolating the underlying PP matrix from flame and oxygen contact. In order to achieve the formation of a continuous dense expanded carbon layer, an IFR loading of no less than 20% is required. For lower IFR loadings, a continuous dense intumescence carbon layer cannot be formed during combustion, greatly reducing the flame retardancy performance. Therefore, IFR loadings of 20%, 25%, and 30% were selected in this study. To improve the fluidity of the IFR-loaded matrix melt, we added 10% by weight of high-melt-flow-index PP (HPP), while the addition of maleic anhydride grafted polypropylene (MAPP) acted as a compatibilizer that increased the compatibility of the PP matrix and IFR. Furthermore, MAPP can also increase the bonding between the PP matrix and glass fibers, further improving the mechanical properties of the prepreg when impregnated with glass fiber.

Flame-retardant PP was prepared by mixing PP with 20, 25, and 30 wt% of IFR using a twin-screw extruder (D: 21.7 mm, L/D: 40, model: KTE-20A, Kerke Extrusion Equipment Co., Ltd., Nanjing, China) at temperatures of 220, 210, 200, 190, 180, and 170 °C. The extruded strands were then cut into pellets. The designation and composition of the various flame-retardant PP samples are listed in Table 1.

**Table 1.** Each group of flame-retardant modified PP.

Samples	IFR (wt%)	BX3900 (wt%)	MF650X (wt%)	MAPP (wt%)
1	0	97	0	3
2	20	77	0	3
3	25	72	0	3
4	30	67	0	3
5	20	67	10	3
6	25	62	10	3
7	30	57	10	3

### 2.3. Preparation of Continuous Glass-Fiber-Reinforced Polypropylene Flame-Retardant Prepreg Tape

The continuous glass-fiber-reinforced polypropylene flame-retardant prepreg was prepared by melt impregnation, with the flame-retardant-modified PP pellets added to a single-screw extruder equipped with a prepreg tape production line, which was designed in our laboratory. The extruder has three heating zones, adjustable to different heating temperatures to control the fluidity of the PP and the impregnation quality of the prepreg tape. The flame-retardant-modified PP melt was extruded into the impregnation die while the continuous glass fiber passed through, so that the continuous glass fiber was impregnated into the flame-retardant PP melt. The continuous glass fiber was drawn through

the dipping die at a specific speed using a pulling device. After rolling and air cooling, the preparation of the continuous glass-fiber-reinforced flame-retardant polypropylene unidirectional prepreg tape was complete.

The temperature of both the extruder and the impregnation die were controlled using a heating device, such that the relationship between the flow and temperature of each flame-retardant-modified PP matrix sample could be varied to prepare prepreg tape at different temperatures.

#### 2.4. Preparation of Unidirectional Laminates and Specimens

Due to heating on the press, the proofing cycle of pressure and cooling was relatively long. In order to improve the preparation efficiency of the laminate, the prepreg tape was stitched into a 320 mm × 120 mm sheet by thermal cutting and welding, and 10 pieces of prepreg tapes were placed between two pieces of equivalently sized 2 mm aluminum plate. In order to prevent the prepreg tape slipping on the aluminum plate after melting, the aluminum plates were fixed with high temperature adhesives and heated by contact with a metal heating block. The heating temperature was set to 220 °C according to the measured temperature and modified PP fluidity relationship of each sample; when the temperature was reached, the aluminum plates were quickly transferred to the press and the pressure set to 5 MPa, which was held for 10 min. After preparation of the laminates, the appropriately sized samples were prepared using an engraving machine according to each test standard.

#### 2.5. Characterization and Testing Methods

##### 2.5.1. Melt Flow Index (MFI)

The MFI is an important parameter for characterizing the viscosity of a thermoplastic resin matrix, and indicates the difficulty of impregnating the fiber with the resin matrix. The resin melt is affected by temperature and the flame retardant loading. The change in resin fluidity can be visually characterized by the MFI, which provides the basic data for determining the process conditions of the melt impregnation preparation of the prepgs. The MFI values were measured using a melt flow indexer (XNR-400 AM, Chengde Baohui Testing Machine Manufacturing Co., Ltd., Chengde, China).

##### 2.5.2. Void Content

The effect of the viscosity of the resin melt on the impregnation quality can be quantified by the porosity of the prepreg. The porosity was measured according to the standard ASTM D2734-16. The theoretical composite density is given by:

$$T_d = \frac{100}{(R/D + r/d)},$$

where  $R$  is the resin in the composite (weight %),  $D$  is the density of the resin,  $r$  is the reinforcement in the composite (weight %), and  $d$  is the density of the reinforcement.

The void content (volume %) can then be calculated by:

$$V = 100 \frac{(T_d - M_d)}{T_d},$$

where  $M_d$  is the measured composite density.

##### 2.5.3. Thermogravimetric Analysis (TGA)

Thermogravimetric analysis (TGA) was conducted on an STA 449F3 (NETZSCH, Dusseldorf, Germany) thermogravimetric analyzer at a heating rate of 10 °C/min in an inert atmosphere of nitrogen with a nitrogen flow rate of 60 mL/min. The mass of each sample was 10 ± 0.5 mg.

#### 2.5.4. The Limit Oxygen Index (LOI)

The LOI measures the minimum oxygen concentration (in a flowing mixture of oxygen and nitrogen gas) required to support candle-like downward flame combustion. An LOI greater than 26 is required to qualify for self-extinguishing. Thus, the LOI serves as a measure of the ease of extinction of a material. The LOI values were measured by an oxygen index meter (Jiangning Analytical Instrument Co., Ltd., Nanjing, China) with sample dimensions of 130 mm × 6.5 mm × 3.0 mm according to the ASTM D2863-19 protocol (Standard Test Method for Measuring the Minimum Oxygen Concentration to Support Candle-Like Combustion of Plastics (Oxygen Index)).

#### 2.5.5. Vertical Burning Tests

Vertical burning tests were conducted using a vertical burning test instrument (YK-Y0142) (Yaoke, Nanjing, China) with sample dimensions of 130 mm × 13 mm × 3.0 mm according to the ASTM D3801-20a protocol (Standard Test Method for Measuring the Comparative Burning Characteristics of Solid Plastics in a Vertical Position).

#### 2.5.6. The Cone Calorimeter Tests (CCT)

Cone calorimeter tests (CCTs) were conducted using a cone calorimeter (Fire Testing Technology, Leeds, UK) with a heat flux of 50 kW/m<sup>2</sup> according to the ISO 5660 standard. The size of each specimen was 100 mm × 100 mm × 3 mm.

#### 2.5.7. Scanning Electronic Microscopy (SEM)

Scanning electron microscopy (SEM) was performed using a JEOL JSM-6010 scanning electron microscope (Japan Electronics Co., Ltd., Tokyo, Japan), to observe the residual char surface of the CGF/PP/IFR samples after cone calorimeter testing. The surface of each specimen was sprayed with a conductive layer of gold before the specimen was tested.

### 3. Results and Discussion

#### 3.1. MFI

The MFI of each of the modified flame-retardant PP samples was compared with the MFI of PP over a range of temperatures. As shown in Figure 1, the flow of resin melt increased with increasing temperature. The effect of the IFR loading on the fluidity of the resin melt can be observed by comparing the different samples with IFR loadings of 20%, 25%, and 30% at each recorded temperature. For PP, PP/20IFR, PP/25IFR, PP/30IFR, MFIs at 180 °C were 48.1, 32.9, 22.1, and 10.9, respectively, while at 230 °C the respective MFIs were 157.5, 110.5, 82.9, and 60.1. Importantly, adding polypropylene with a high melt index effectively improved the fluidity of the melt; the MFIs of the PP matrixes containing HPP, PP/20IFR/HPP, PP/25 IFR/HPP and PP/30 IFR/HPP were 63.3, 49.5 and 40.1 at 180 °C, and 138.7, 123.4 and 103.1 at 230 °C, respectively. The changes in MFI with the addition of HPP clearly indicate that HPP can effectively improve the MFI and partially counteract the rise in melt viscosity caused by the addition of IFR. Therefore, the improved fluidity, combined with the temperature control, can regulate the viscosity of the resin melt to ensure impregnation. This is discussed below, along with the porosity test results for different prepreg compositions.

#### 3.2. Void Content

The porosities, at different temperatures, of the prepgs prepared using each group of matrixes can be seen in Figure 2. According to comparison of the MFI values between different flame-retardant-modified PP samples, and our previous experience in prepreg tape preparation, resin melt with an MFI above 60 can stabilize the continuous preparation of the pre-immersion belt. When the MFI was below 60, the melt fluidity was not sufficiently high, therefore impregnating the fiber was more difficult. During the roller pressing process, holes appeared on the surface of the prepreg tape from time to time such that it was not possible to prepare a high-quality qualified prepreg. This can be seen in our experiments,

where continuous quality-stable prepreg tape could not be prepared with PP/25IFR at 200 °C, nor with PP/30IFR at 200, 210, or 220 °C, although a pre-immersion belt could be prepared with a temperature of 230 °C. However, the porosity of the prepared material was 6.70%, while the prepreg tape prepared with PP/30IFR/HPP had a porosity of only 3.62% at the same temperature.

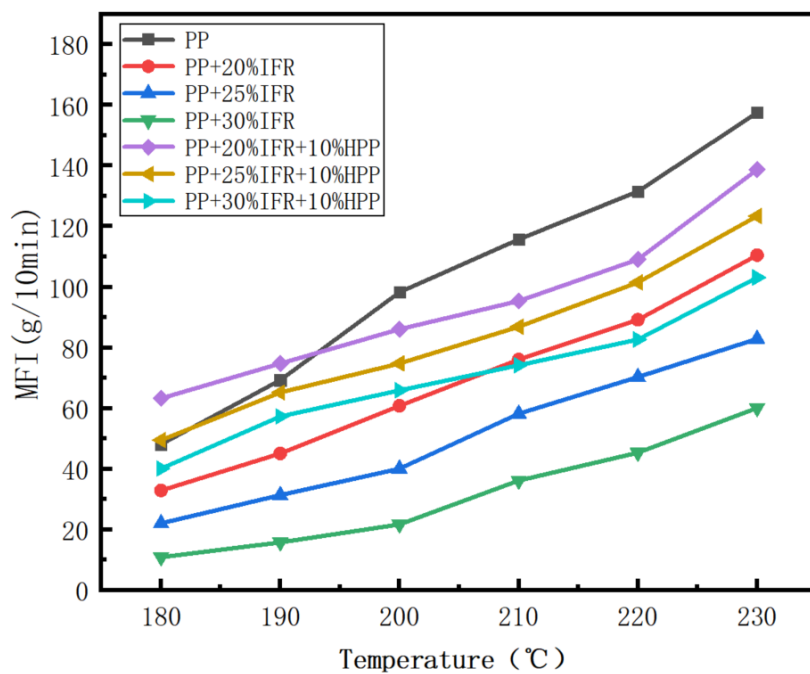


**Figure 1.** MFI of each group of flame-retardant-modified PP varies with temperature.

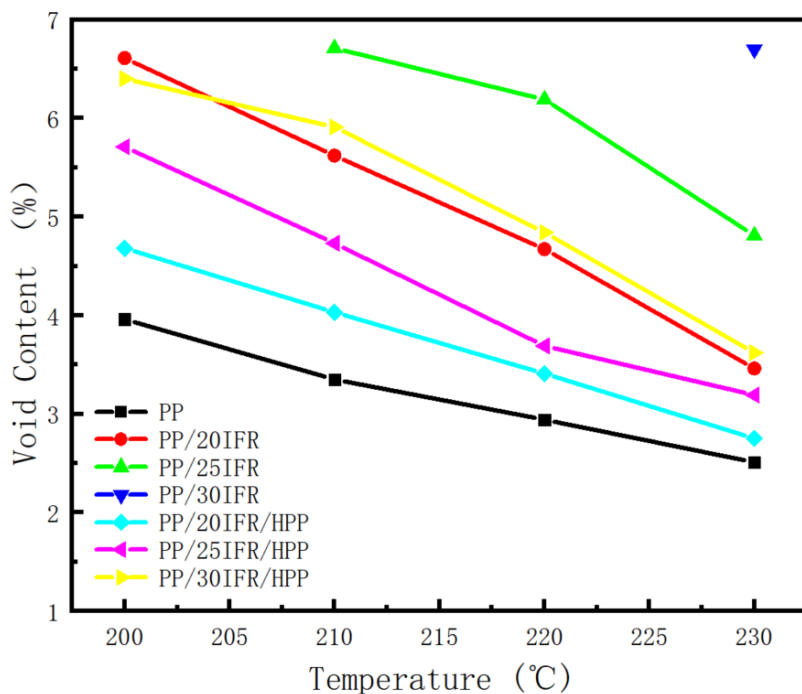


**Figure 2.** The porosity at different temperatures of the prepreg prepared using each group of matrixes.

### 3.3. Thermal Properties

To investigate the effects of flame retardants on CGF/PP, the thermal properties and the amount of residual char obtained from the CGF/PP and CGF/PP/IFR samples

were compared by TGA testing in an N<sub>2</sub> atmosphere. The CGF/PP and CGF/PP/IFR TGA curves are shown in Figure 3. The detailed data are listed in Table 2. The CGF/PP sample began to decompose at 419 °C, and the mass did not change beyond 490 °C, which was attributed to the remnant glass fiber. Compared to the CGF/PP sample, the CGF/PP/20IFR/HPP, CGF/PP/25IFR/HPP, and CGF/PP/30IFR/HPP samples did not decompose completely. The remaining residual carbon layer acted as an insulation barrier, increasing the thermal stability of the material system. The CGF/PP/IFR/HPP samples had similar TGA curves below 250 °C, but the mass of residual char increased with increased IFR loading above 400 °C, with the CGF/PP/20IFR/HPP, CGF/PP/25IFR/HPP, and CGF/PP/30IFR/HPP samples retaining up to 42.0, 46.7, and 48.7% char residue at 700 °C, respectively. The temperature corresponding to a 5% sample weight loss is defined here as the onset decomposition temperature, T<sub>onset</sub>. As shown in Figure 3 and Table 2, the addition of IFRs slightly decreased the onset decomposition temperatures of CGF/PP. The onset temperatures, T<sub>onset</sub>, for CGF/PP, CGF/PP/20IFR/HPP, CGF/PP/25IFR/HPP, and CGF/PP/30IFR/HPP were 419, 414, 404, and 387 °C, respectively. It can be seen that when the amount of IFR increased, T<sub>onset</sub> decreased, which was attributed to the decomposition temperature of the IFR being lower than the PP decomposition temperature. Importantly, heat absorption during the decomposition of the IFR protected the PP matrix.

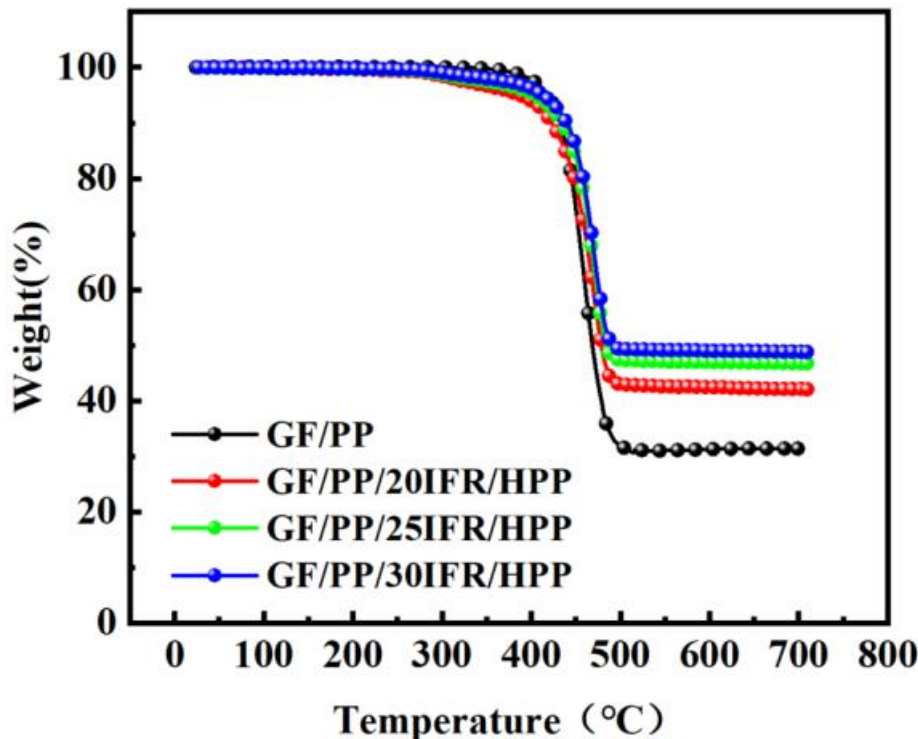


**Figure 3.** The TG curves of the samples in N<sub>2</sub>.

**Table 2.** Thermal decomposition properties of CGF/PP and CGF/PP/IFR/HPP samples in N<sub>2</sub>.

Samples	T5% (°C)	T10% (°C)	T20% (°C)	T50% (°C)	Residual Weight (wt%)
CGF/PP	419	433	445	468	31.4
CGF/PP/20IFR/HPP	414	440	458	491	42.0
CGF/PP/25IFR/HPP	404	434	455	484	46.7
CGF/PP/30IFR/HPP	387	423	448	478	48.7

### 3.4. Flame Retardancy and Burning Behaviors

To explore the flame retardancy of the CGF/PP and CGF/PP/IFR/HPP samples, the LOI values and vertical burning ratings (UL-94) of the CGF/PP and CGF/PP/IFR/HPP

samples with different IFR loadings were measured, and the results are presented in Figure 4 and Table 3. The GF/PP samples exhibited an LOI value of 20.5 and there was no rating from the UL-94 test (see Figure 3), while the LOI values of the CGF/PP/20IFR, CGF/PP/25IFR, and CGF/PP/30IFR samples were 31.9, 34.3 and 36.4, corresponding to increases of 55.6%, 67.3% and 77.5%, respectively.

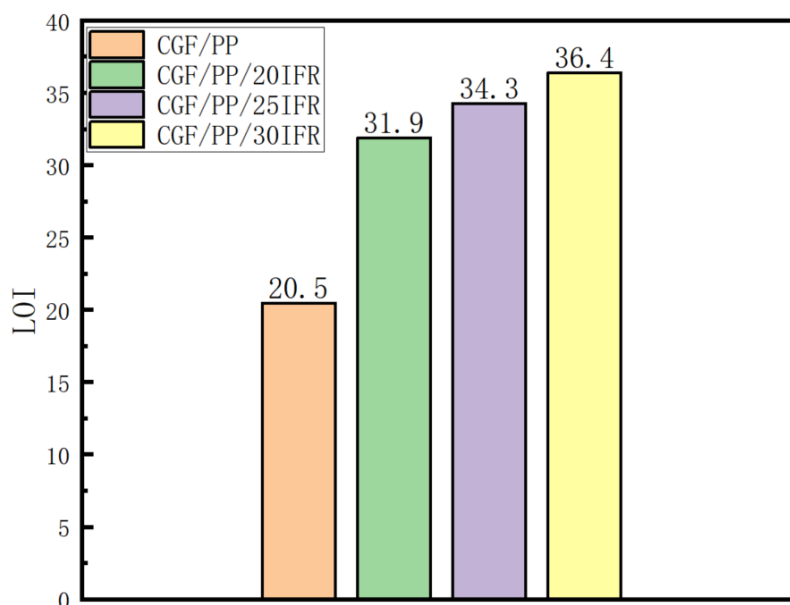


**Figure 4.** The LOI of samples with different content of IFR.

**Table 3.** UL-94 results of CGF/PP and CGF/PP/IFR samples.

Sample	UL-94 Rating	Dripping
CGF/PP	No rating	No
CCF/PP/20IFR	V1	No
CCF/PP/25IFR	V0	No
CCF/PP/30IFR	V0	No

The UL-94 ratings of the CGF/PP, CGF/PP/20IFR, CGF/PP/25IFR, and CGF/PP/30IFR samples were, respectively: not rated, V1, V0, and V0. None of the samples exhibited dripping. With an increase in the IFR content, the self-extinguishing time of the sample was significantly reduced.

### 3.5. CCT Results and Discussion

CCT has been proven to be an effective procedure for evaluating fire hazards. To measure the effects of IFR loading on the flame retardancy of the GF/PP/IFR/HPP composites, CCTs with a heat flux of  $50\text{ kW/m}^2$  were conducted. CCT can provide many important parameters, including time to ignition (TTI), heat release rate (HRR), total heat release (THR), peak heat release rate (PHRR), time to peak heat release rate (TPHRR), smoke production rate (SPR), peak smoke production rate (PSPR), total smoke production (TSP), the fire performance index (FPI), and the fire growth index (FGI), all of which can be calculated from the CCT measurements.

HRR is believed to be one of the most important parameters for quantifying fire hazards. Figure 5 shows the HRR curves for each sample, and the combustion parameters are listed in Table 4. As shown in Figure 5, the CGF/PP samples had a sharp PHRR, reaching  $519.1\text{ kW/m}^2$ . The TPHRR was 55 s, while the HRR curves of the CGF/PP/IFR/HPP samples were largely decreased; the PHRRs of the CGF/PP/20IFR/HPP, CGF/PP/25IFR/HPP, and CGF/PP/30IFR/HPP samples were  $159.5$ ,  $117.4$  and  $101.1\text{ kW/m}^2$ , corresponding to a decrease of 69.3%, 77.4% and 80.5%, respectively, and their respective TPHRRs were

46, 59 and 76 s. Thus, TPHRR increased with increasing IFR content. Notably, the TPHRR of CGF/PP/20IFR/HPP (46 s) was shorter than that of CGF/PP (55 s) because the addition of IFR decreased the PP decomposition temperature, which is consistent with the TGA results. The TTI of the CGF/PP, CGF/PP/20IFR/HPP, CGF/PP/25IFR/HPP, and CGF/PP/30IFR/HPP samples were 23, 20, 18 and 19 s, respectively. The same conclusion can be drawn, that lower IFR loading reduced the decomposition temperature of the samples, leading to shorter TTI. Beyond a certain IFR content, the TTI increased with increasing IFR content. It is shown in Figure 6 that the THRs of CGF/PP, CGF/PP/20IFR/HPP, CGF/PP/25IFR/HPP, and CGF/PP/30IFR/HPP samples were 176.7, 104.7, 85.4 and 71.5 MJ/m<sup>2</sup>, respectively. Thus, with increasing IFR content, THR decreased by 59.2, 48.3 and 40.5%, respectively, indicating that the addition of IFR effectively reduced THR.

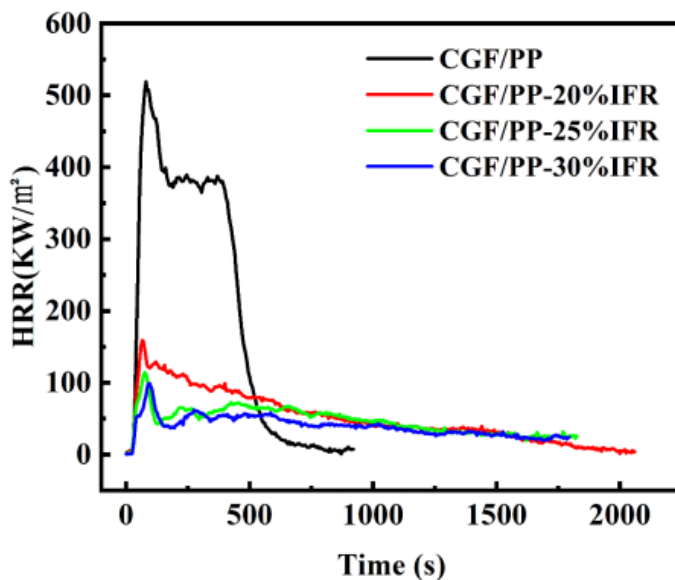


**Figure 5.** Heat release rate curves of composites with different IFR content.

**Table 4.** Combustion parameters of samples from cone calorimeter tests.

Samples	TTI (s)	TPHRR (s)	PHRR (kw/m <sup>2</sup> )	THR (MJ/m <sup>2</sup> )	PSPR (m <sup>2</sup> /S)	TSP (m <sup>2</sup> )	FPI (sm <sup>2</sup> /kW)	FGI (kW/sm <sup>2</sup> )
CGF/PP	23	55	519.1	176.7	0.039	13.72	0.044	9.438
CGF/PP-20%IFR	20	46	159.5	104.7	0.018	5.53	0.125	3.467
CGF/PP-25%IFR	18	59	117.4	85.4	0.010	4.08	0.153	1.990
CGF/PP-30%IFR	19	76	101.1	71.5	0.007	3.71	0.188	1.330

FPI is defined as the ratio of TTI to PHRR. Many studies have shown that it has a certain correlation with the time taken for a fire in a closed space (such as indoors) to reach the critical point of flashover, i.e., the “flashover time.” The flashover time value is an important parameter in fire protection engineering design. In particular, it is an important parameter required for calculating fire escape times. The FPI values of the CGF/PP, CGF/PP/20IFR/HPP, CGF/PP25IFR/HPP, and CGF/PP30IFR/HPP samples were 0.044, 0.125, 0.153 and 0.188 s·m<sup>2</sup>/kW, respectively. The FGI is defined as the ratio of PHRR to TPHRR. The FGI reflects the ability of a material to react to heat. A larger FGI indicates that once the material is exposed to an excessively strong thermal environment, it can ignite quickly and cause the fire to spread rapidly. Therefore, the greater the FGI of a material, the greater its fire risk. The FGI values of the CGF/PP, CGF/PP/20IFR/HPP, CGF/PP/25IFR/HPP, and CGF/PP/30IFR/HPP samples were 9.438, 3.467, 1.990 and 1.330 kW/s·m<sup>2</sup>, respectively. After addition of IFR, the

FGI of the samples decreased rapidly, indicating a significant decline in fire hazard transmission capacity.

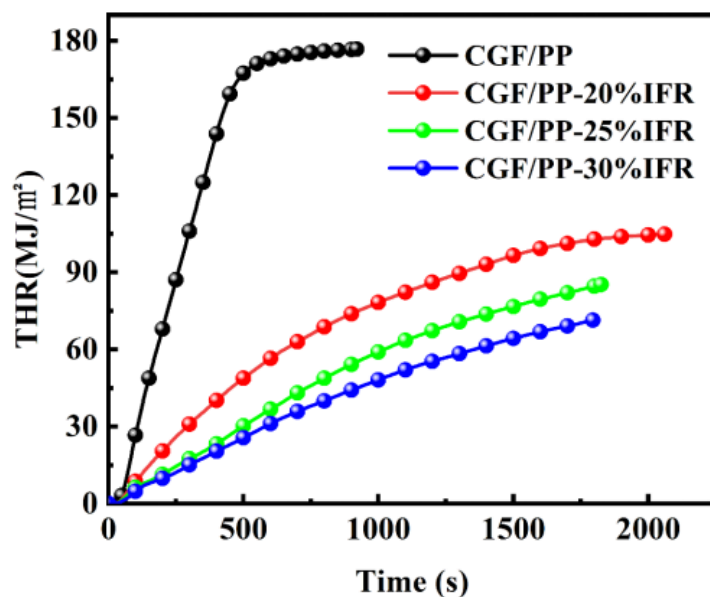


**Figure 6.** Total heat release rate curves of composites with different IFR content.

While the effect of flame retardants on the heat release performance of the composites during combustion has been discussed, we note that there are two aspects to assessing fire hazard: thermal hazard (discussed above), and non-thermal hazards, such as whether the product is poisonous or corrosive, or its smoke production. Thus, here we discuss the non-thermal hazards associated with the CGF/PP-based samples with various IFR loadings. The SPR curves are shown in Figure 7 and TSP curves are shown in Figure 8. The pure CGF/PP samples had a higher SPR, reaching a peak of  $0.041 \text{ m}^2/\text{s}$ , with the curve dropping sharply at approximately 500 s, which is consistent with the HRR curve from the CGF/PP sample. The curves of the CGF/PP/IFR samples decreased sharply. The PSPRs of the CGF/PP/20IFR/HPP, CGF/PP/25IFR/HPP, and CGF/PP/30/IFR/HPP samples were  $0.018$ ,  $0.010$  and  $0.007 \text{ m}^2/\text{s}$ , respectively.

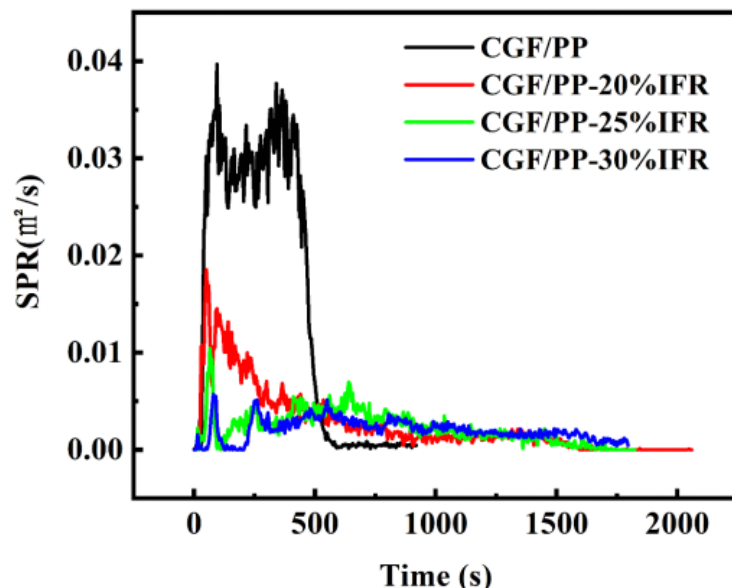


**Figure 7.** Smoke production rate curves of composites with different IFR content.

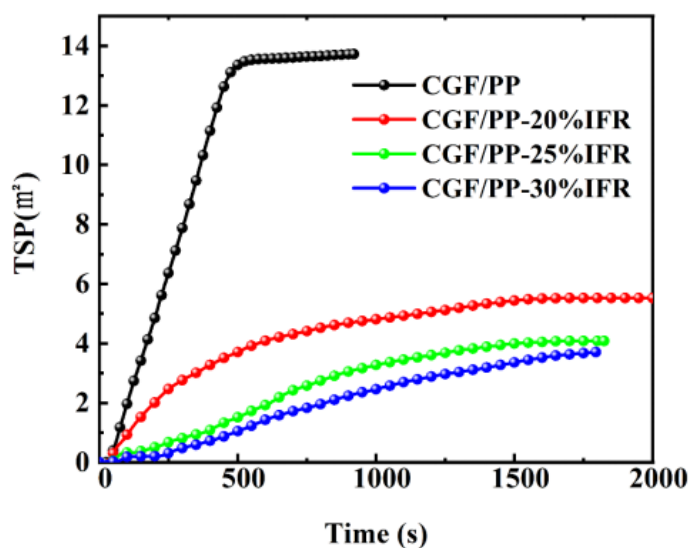


**Figure 8.** Total smoke production rate curves of composites with different IFR content.

### 3.6. The Morphology Analysis of Residual Char after the CCT

Photographs taken after the CCT are shown in Figures 9 and 10. In the case of no added flame retardant, there was no carbon residue, with only the glass fibers remaining, and the sample did not expand. With the addition of flame retardant, the sample expanded significantly. The expansion thickness of the carbon layer reached 14.1, 15.1 and 26.2 mm, as shown in Figure 10. The function of the expanded carbon layer was to provide heat insulation and prevent exposure to air. Considering the heat release data along with results from previous studies, if we compare the expanded carbon layer corresponding to different flame retardant loadings, we find that the density of the expanded carbon layer increased with increasing content of flame retardant, such that the exposed area of the fiber decreased, the thickness of the expanded carbon layer increased, and the heat insulation and air barrier properties of the carbon layer increased so that the heat and the amount of smoke produced by the material were reduced. An SEM image is shown in Figure 11. In the absence of a flame retardant, the matrix completely burned away, leaving a smooth fiber surface. With the addition of flame retardant, a carbon residue was observed attached to the fiber surface. As the amount of char residue increased, it eventually formed an obvious carbon layer covering the fiber in the CGF/PP/30IFR sample. Therefore, the addition of IFR solved the candlewick effect caused by the fibers.

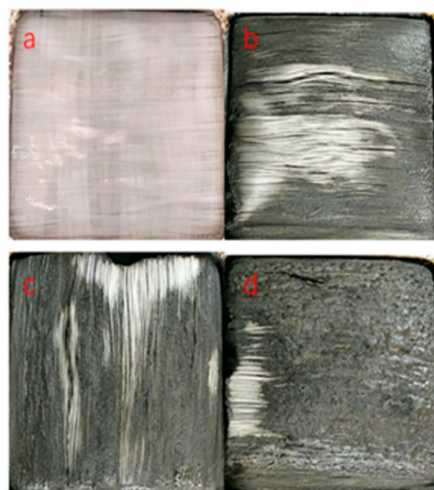


**Figure 9.** Front view digital photographs of residues after cone calorimeter testing (a) CGF/PP (b) CGF/PP/20IFR/HPP (c) CGF/PP/25IFR/HPP (d) CGF/PP/30IFR/HPP.

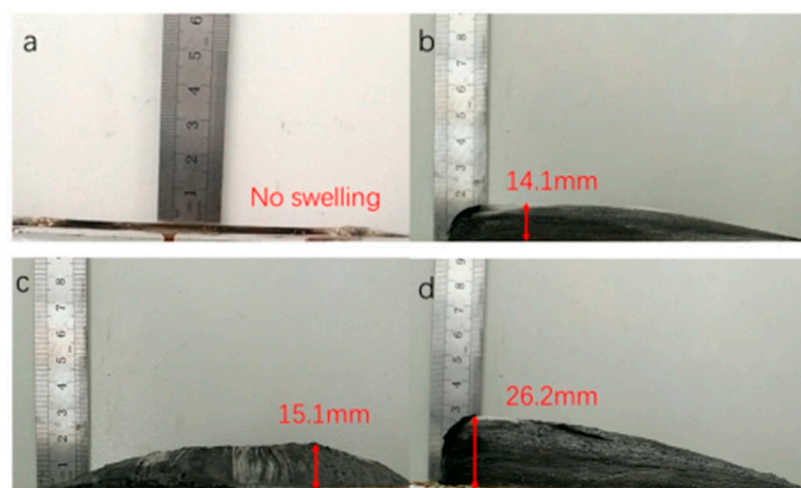


**Figure 10.** Side view digital photographs of residues after cone calorimeter testing, (a) CGF/PP (b) CGF/PP/20IFR/HPP (c) CGF/PP/25IFR/HPP (d) CGF/PP/30IFR/HPP.

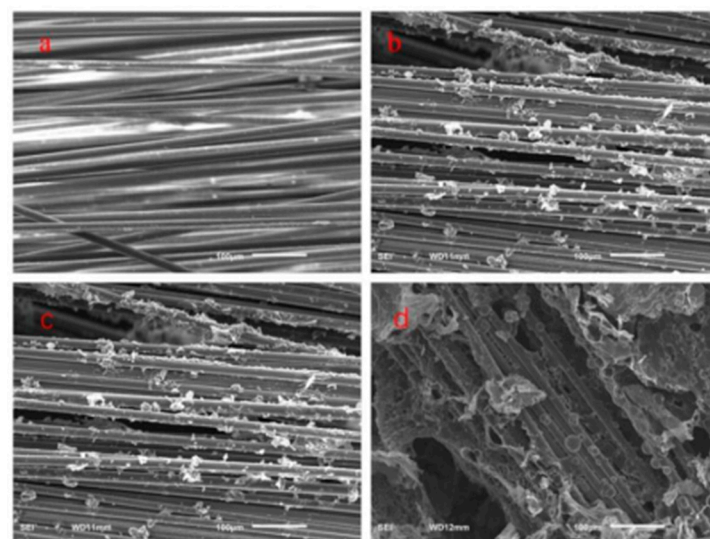


**Figure 11.** SEM images after cone calorimeter testing of (a) CGF/PP (b) CGF/PP/20IFR/HPP (c) CGF/PP/25IFR/HPP (d) CGF/PP/30IFR/HPP.

#### 4. Conclusions

Through the analysis and discussion of the experimental results, we can draw the following conclusions:

The addition of IFR increased the PP melt viscosity, and the addition of 10 wt% HPP compensated for this by significantly reducing the melt viscosity of the PP matrix, to ensure the feasibility of the melt impregnation method for preparing the prepeg.

The addition of IFR slightly reduced the thermal decomposition temperature of the PP matrix, because the thermal decomposition temperature of the IFR was lower than the thermal decomposition temperature of PP; consequently, when the composites were thermally affected, the IFR decomposed, absorbed heat, released gas, and played a role in protecting the PP matrix.

With increasing flame retardant content, the tightness and thickness of the residue char layers increased, greatly improving the flame-retardant performance and significantly decreasing the heat release rate, total heat release, and the amount of smoke.

Considering the economic cost and use requirements of the composites, it was demonstrated that an IFR loading of 25% in the CGF/PP composite attained a V0 UL-94 rating.

**Author Contributions:** Data curation, Writing—original draft, Writing—review and editing Y.S.; Methodology, Project administration, Resources, Supervision, J.L.; review, Project administration, Supervision H.L. All authors have read and agreed to the published version of the manuscript.

**Funding:** This work was supported by Fundamental Research Funding (No. 514010104-302) and National Natural Science Foundation of China (Grant No. 11872086).

**Institutional Review Board Statement:** Not applicable.

**Informed Consent Statement:** Not applicable.

**Data Availability Statement:** Not applicable.

**Conflicts of Interest:** The authors declare no conflict of interest.

## References

1. Vaidya, U. Thermoplastic Composites for Aerospace Applications. *Aeronaut. Manuf. Technol.* **2015**, *14*, 69–71.
2. Gibson, A.G.; Torres, M.O.; Browne, T.N.A.; Feih, S.; Mouritz, A.P. High temperature and fire behaviour of continuous glass fibre/polypropylene laminates. *Compos. Part A Appl. Sci. Manuf.* **2010**, *41*, 1219–1231. [[CrossRef](#)]
3. Correia, J.R.; Bai, Y.; Keller, T. A review of the fire behaviour of pultruded GFRP structural profiles for civil engineering applications. *Compos. Struct.* **2015**, *127*, 267–287. [[CrossRef](#)]
4. Li, D.P.; Li, C.X.; Jiang, X.L.; Liu, T.; Zhao, L. Synergistic effects of intumescence flame retardant and nano-CaCO<sub>3</sub> on foamability and flame-retardant property of polypropylene composites foams. *J. Cell. Plast.* **2018**, *54*, 615–631. [[CrossRef](#)]
5. Zhao, Z.L.; Jin, Q.; Zhang, N.E.; Guo, X.R.; Yan, H. Preparation of a novel polysiloxane and its synergistic effect with ammonium polyphosphate on the flame retardancy of polypropylene. *Polym. Degrad. Stab.* **2018**, *150*, 73–85. [[CrossRef](#)]
6. Shen, H.Y.; Liu, Y.Z. One-step synthesis of hydrophobic magnesium hydroxide nanoparticles and their application in flame-retardant polypropylene composites. *Chin. J. Chem. Eng.* **2018**, *26*, 2199–2205. [[CrossRef](#)]
7. Ren, Y.; Yuan, D.D.; Li, W.M.; Cai, X.F. Flame retardant efficiency of KH-550 modified urea-formaldehyde resin cooperating with ammonium polyphosphate on polypropylene. *Polym. Degrad. Stab.* **2018**, *151*, 160–171. [[CrossRef](#)]
8. Zhao, P.P.; Guo, C.G.; Li, L.P. Exploring the effect of melamine pyrophosphite and aluminum hypophosphite on flame retardant wood flour/polypropylene composites. *Constr. Build. Mater.* **2018**, *170*, 193–199. [[CrossRef](#)]
9. Chen, H.D.; Wang, J.H.; Ni, A.Q.; Ding, A.X.; Han, X.; Sun, Z.H. The Effects of a Macromolecular Charring Agent with Gas Phase and Condense Phase Synergistic Flame Retardant Capability on the Properties of PP/IFR Composites. *Materials* **2018**, *11*, 111. [[CrossRef](#)]
10. Zhao, W.; Kumar Kundu, C.; Li, Z.; Li, X.; Zhang, Z. Flame retardant treatments for polypropylene: Strategies and recent advances. *Compos. Part A Appl. Sci. Manuf.* **2021**, *145*, 106382. [[CrossRef](#)]
11. Zhu, J.Q.; Lu, X.; Yang, H.Y.; Xin, Z. Vinyl polysiloxane microencapsulated ammonium polyphosphate and its application in flame retardant polypropylene. *J. Polym. Res.* **2018**, *25*, 107. [[CrossRef](#)]
12. Zhu, C.J.; He, M.S.; Cui, J.G.; Tai, Q.L.; Song, L.; Hu, Y. Synthesis of a novel hyperbranched and phosphorus-containing charring-foaming agent and its application in polypropylene. *Polym. Adv. Technol.* **2018**, *29*, 2449–2456. [[CrossRef](#)]
13. Zhu, C.J.; He, M.S.; Liu, Y.; Cui, J.G.; Tai, Q.L.; Song, L.; Hu, Y. Synthesis and application of a mono-component intumescence flame retardant for polypropylene. *Polym. Degrad. Stab.* **2018**, *151*, 144–151. [[CrossRef](#)]
14. Bazan, P.; Salasińska, K.; Kuciel, S. Flame retardant polypropylene reinforced with natural additives. *Ind. Crops Prod.* **2021**, *164*, 113356. [[CrossRef](#)]
15. Dasari, A.; Yu, Z.-Z.; Cai, G.-P.; Mai, Y.-W. Recent developments in the fire retardancy of polymeric materials. *Prog. Polym. Sci.* **2013**, *38*, 1357–1387. [[CrossRef](#)]
16. Qin, Y.; Li, M.; Huang, T.; Shen, C.; Gao, S. A study on the modification of polypropylene by a star-shaped intumescence flame retardant containing phosphorus and nitrogen. *Polym. Degrad. Stab.* **2022**, *195*, 109801. [[CrossRef](#)]
17. Lin, Q.; Ferriol, M.; Cochez, M.; Vahabi, H.; Vagner, C. Continuous fiber-reinforced thermoplastic composites: Influence of processing on fire retardant properties. *Fire Mater.* **2017**, *41*, 646–653. [[CrossRef](#)]
18. Kim, N.K.; Bhattacharyya, D. Development of fire resistant wool polymer composites: Mechanical performance and fire simulation with design perspectives. *Mater. Des.* **2016**, *106*, 391–403. [[CrossRef](#)]
19. Chen, H.D.; Wang, J.H.; Ni, A.Q.; Ding, A.X.; Sun, Z.H.; Tao, S.L. Effect of an intumescence flame retardant on the fracture toughness (Mode I), thermal, and flame-retardant properties of continuous glass fibre-reinforced polypropylene composites. *Plast. Rubber Compos.* **2018**, *47*, 113–121. [[CrossRef](#)]
20. Chen, H.D.; Wang, J.H.; Ni, A.Q.; Ding, A.X.; Sun, Z.H.; Han, X. Effect of novel intumescence flame retardant on mechanical and flame retardant properties of continuous glass fibre reinforced polypropylene composites. *Compos. Struct.* **2018**, *203*, 894–902. [[CrossRef](#)]
21. Liu, L.; Liu, Y.S.; Han, Y.; Liu, Y.; Wang, Q. Interfacial charring method to overcome the wicking action in glass fiber-reinforced polypropylene composite. *Compos. Sci. Technol.* **2015**, *121*, 9–15. [[CrossRef](#)]

22. Zhou, Y.; He, W.D.; Wu, Y.F.; Xu, D.H.; Chen, X.L.; He, M.; Guo, J.B. Influence of thermo-oxidative aging on flame retardancy, thermal stability, and mechanical properties of long glass fiber-reinforced polypropylene composites filled with organic montmorillonite and intumescent flame retardant. *J. Fire Sci.* **2019**, *37*, 176–189. [[CrossRef](#)]
23. Zhou, D.F.; He, W.D.; Wang, N.; Chen, X.L.; Guo, J.B.; Ci, S.T. Effect of thermo-oxidative aging on the mechanical and flame retardant properties of long glass fiber-reinforced polypropylene composites filled with red phosphorus. *Polym. Compos.* **2018**, *39*, 2634–2642. [[CrossRef](#)]
24. Xu, J.Y.; Li, K.D.; Deng, H.M.; Lv, S.; Fang, P.K.; Liu, H.; Shao, Q.; Guo, Z.H. Preparation of MCA-SiO<sub>2</sub> and Its Flame Retardant Effects on Glass Fiber Reinforced Polypropylene. *Fibers Polym.* **2019**, *20*, 120–128. [[CrossRef](#)]
25. Luo, X.; He, M.; Guo, J.B.; Zhang, K.Z.; Wu, B. Brominated flame retardant composed of decabromodiphenyl oxide and antimonous oxide flame retardant for long glass fiber-reinforced polypropylene. *J. Thermoplast. Compos. Mater.* **2015**, *28*, 1373–1386. [[CrossRef](#)]
26. Khosravani, M.R. Composite Materials Manufacturing Processes. *Appl. Mech. Mater.* **2011**, *110–116*, 1361–1367. [[CrossRef](#)]
27. Wang, C.; Yue, G.; Bai, G.; Pan, L.; Zhang, B. Compaction behavior and permeability property tests of preforms in vacuum-assisted resin transfer molding using a combined device. *Measurement* **2016**, *90*, 357–364. [[CrossRef](#)]
28. Mitschang, P.; Blinzler, M.; Wöglinger, A. Processing technologies for continuous fibre reinforced thermoplastics with novel polymer blends. *Compos. Sci. Technol.* **2003**, *63*, 2099–2110. [[CrossRef](#)]
29. Trende, A.; Åström, B.T.; Wöglinger, A.; Mayer, C.; Neitzel, M. Modelling of heat transfer in thermoplastic composites manufacturing: Double-belt press lamination. *Compos. Part A Appl. Sci. Manuf.* **1999**, *30*, 935–943. [[CrossRef](#)]
30. Wang, Y.; Dong, Q.; Liu, X. Mode 1 Interlaminar Fracture Behaviour of Continuous Glass Fibre/ Polypropylene Composites Based on Commingled Yarn. *Polym. Polym. Compos.* **2006**, *15*, 229–239. [[CrossRef](#)]
31. Fang, J.; Zhang, L.; Li, C. The combined effect of impregnated rollers configuration and glass fibers surface modification on the properties of continuous glass fibers reinforced polypropylene prepreg composites. *Compos. Sci. Technol.* **2020**, *197*, 108259. [[CrossRef](#)]
32. Kiss, P.; Stadlbauer, W.; Burgstaller, C.; Archodoulaki, V.-M. Development of high-performance glass fibre-polypropylene composite laminates: Effect of fibre sizing type and coupling agent concentration on mechanical properties. *Compos. Part A Appl. Sci. Manuf.* **2020**, *138*, 106056. [[CrossRef](#)]
33. Lebrun, G.; Bureau, M.N.; Denault, J. Thermoforming-Stamping of Continuous Glass Fiber/Polypropylene Composites: Interlaminar and Tool-Laminate Shear Properties. *J. Thermoplast. Compos. Mater.* **2016**, *17*, 137–165. [[CrossRef](#)]
34. Thomason, J.L. Glass fibre sizing: A review. *Compos. Part A Appl. Sci. Manuf.* **2019**, *127*, 105619. [[CrossRef](#)]